Mem. S.A.It. Suppl. Vol. 14, 67

Memorie della
Supplementi

A new kinematic survey to study the stellar populations of the Milky Way

Based on GSC-II and SDSS-DR7

A. Spagna[1], B. Bucciarelli[1], M.G. Lattanzi[1], P. Re Fiorentin[2], and R. Smart[1]

[1] Istituto Nazionale di Astrofisica – Osservatorio Astronomico di Torino, Via Osservatorio 20, I-10025 Torino, Italy, e-mail: [spagna;bucc;lattanzi;smart]@oato.inaf.it
[2] University of Ljubljana, Faculty of Mathematics and Physics, Jadranska 19, SLO-1000 Ljubljana, Slovenia, e-mail: paola.refiorentin@fmf.uni-lj.si

Abstract. We present a new catalog which includes high-quality proper motions for 77 million objects down to $r \approx 20$ from the Seventh Data Release of the Sloan Digital Sky Survey combined with multiepoch positions from the database used for the construction of the Guide Star Catalog II. Thanks to the wide time baseline, spanning more than 50 years, proper motions reach a precision of 3 mas^{-1} yr.
By means of the SDSS photometric and spectroscopic data, which include radial velocities and stellar atmospheric parameters (effective temperature, surface gravity, and metallicity), we also estimate photometric distances and 3D velocities for a sample of 27 000 FGK dwarfs that we adopted as tracers of the Milky Way stellar populations within a few kiloparsecs from the Sun.
The properties of this new GSCII-SDSS-based catalog, as well as preliminary results of its application to the study of the galactic disk and halo, are presented.

Key words. Surveys – Methods: statistical – Galaxy: abundances – Galaxy: stellar content – Galaxy: kinematics and dynamics

1. Introduction

Wide field surveys are fundamental for the study of the formation and evolution of the Milky Way. In particular, spatial and velocity distributions, and the chemical abundances of selected galactic tracers can be derived from stellar surveys which integrate astrometric, photometric, and spectroscopic data.

Send offprint requests to: A. Spagna

Here, we present a new kinematic catalog derived by assembling the astrometric data from the Second Guide Star Catalog (GSC-II; Lasker et al. 2008) with spectro-photometric data from the Seventh Data Release of the Sloan Digital Sky Survey (SDSS DR7; e.g. Abazajian et al. 2009; Yanny et al. 2009).

The following material has been used:

- SDSS-DR7 *imaging* survey, which contains positions, classification, and *ugriz*

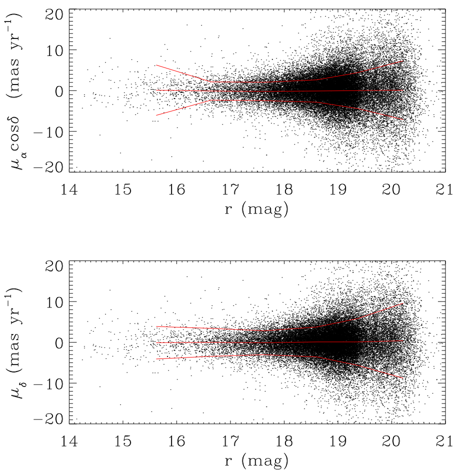

Fig. 1. Proper motions of a QSO sample from the LQRF (*dots*) as a function of the r magnitude. The central solid line marks the mean proper motion, while the external ones trace the boundary lines at $\pm 1\sigma$.

photometry for 357 million objects over 11 663 square-degrees.
- SDSS-DR7 *spectroscopic* survey, with moderate resolution ($R \approx 1800$) stellar spectra covering the wavelength range 3850–9000 Å for approximately 300 000 stars in the magnitude range $14.0 \leq g \leq 20.5$; all this allows to derive radial velocities good to $10\,\mathrm{km\,s^{-1}}$ and atmospheric parameters (e.g. $T_{\rm eff}$, $\log g$, [Fe/H]).
- GSC-II database which includes multi-epoch positions, classification, and multi-band photographic photometry for about 1 billion objects over the whole sky.

2. The proper motion catalog

By applying a cross-matching searching radius of 3″, we found 110 million sources in common between GSC-II and SDSS. Proper motions could be computed for 77 million sources by combining SDSS second-epoch positions with the multi-epoch positions derived from the GSC-II database. Typically, for each source, 5-10 observations are available, spanning a time baseline of ≈ 50 years.

According to Pier et al. (2003), the precision of the SDSS positions is about 45 mas or 75 mas, when reduced against UCAC2 or Tycho2, respectively. Systematic errors are estimated in the range of 20-30 mas. The GSC-II absolute position accuracy is about 0.2″ – 0.3″, including systematic errors of about 0.1″. However, relative astrometry is significantly better and attains a precision of 0.1″, consistent with the centroid error of the photographic images. Thus, we adopted the more accurate SDSS system as reference frame and proper motions were computed by converting the original GSC-II plate coordinates, (X, Y), to this reference frame as follows:

1. we divided the area covered by the survey in regions of 0.21 square-degrees, defined by a HEALPix[1] sky tessellation of level 7;
2. for each region, second order polynomial transformations, $\xi = f(X, Y)$, $\eta = g(X, Y)$, from the GSC-II plate coordinates (X,Y) to the SDSS standard coordinates, (ξ, η), were computed for each overlapping plate; the transformation coefficients were computed by means of best-fits based on a set of reference stars with $17 < r < 18$, selected within a 30″-radius circle circumscribed around the HEALPix;
3. *relative* proper motions, $\mu_\xi \equiv \mu_\alpha \cos\delta$, $\mu_\eta \equiv \mu_\delta$ are then derived through a linear fit to the time-spaced positions;
4. finally, *absolute* proper motions are obtained by removing the zero-point estimated as the mean motion of the extragalactic sources in the field.

Proper motion formal errors vary as a function of magnitude and are typically in the range 2-3 mas yr^{-1} at intermediate magnitudes, $16 < r < 18.5$. As shown in Fig. 1, these values are also consistent with the results of an external comparison against a subsample of 77 000 QSOs from the Large Quasar Reference Frame (LQRF) catalog assembled by Andrei et al. (2009). The mean proper motion is close to zero, as expected for extragalac-

[1] Description and references on the HEALPix sky tessellation are available at http://healpix.jpl.nasa.gov/

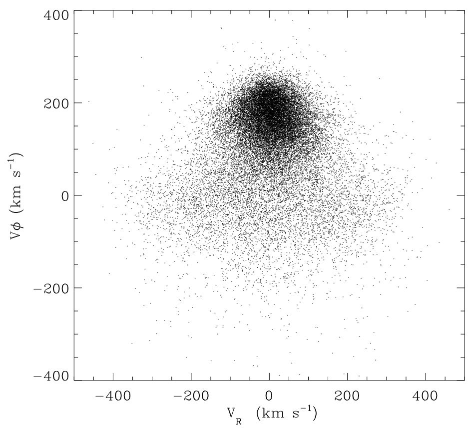

Fig. 2. Velocity distribution, V_ϕ vs. V_R of the kinematic sample.

tic sources, while the dispersion represents the proper motion error.

SDSS also provides proper motions which have been computed combining SDSS and USNO-B positions as described by Munn et al. (2003). Comparisons against the same QSO sample indicate that the accuracy of the two catalogs is comparable.

Table 1. Mean velocities and dispersions in kms^{-1} of two metallicity samples, -0.7 <[Fe/H]< -0.5 and [Fe/H]< -1.8, representative of the thick disk and halo, respectively. Parameter errors are reported in brackets.

z (kpc)	V_R	V_ϕ	V_Z (km s^{-1})	σ_{V_R}	σ_{V_ϕ}	σ_{V_Z}
			-0.7 < [Fe/H] < -0.5			
1.0-1.5	3	180	1	49	43	39
	(1)	(1)	(0.2)	(1)	(1)	(0.2)
1.5-2.5	1	165	3	60	49	43
	(1)	(1)	(1)	(1)	(1)	(1)
2.5-3.0	5	147	3	75	59	45
	(3)	(3)	(1)	(3)	(3)	(1)
			[Fe/H] < -1.8			
1.0-1.5	3	32	2	127	107	84
	(4)	(5)	(3)	(5)	(5)	(3)
1.5-2.5	-4	18	-7	131	99	91
	(4)	(3)	(3)	(4)	(3)	(3)
2.5-3.0	29	19	4	140	94	102
	(9)	(3)	(5)	(9)	(3)	(5)

3. The (sub)dwarf sample

Spectroscopic parameters ($T_{\rm eff}$, log g, [Fe/H], and V_r) are available for 151 000 sources of the proper motion catalog. From this sample, we selected sources with 4500 K< $T_{\rm eff}$ < 7500 K and $\log g$ > 3.5 corresponding to FGK (sub)dwarfs to be used as tracers of the inner halo and thick disk. Photometric distances have been derived by means of Equation 1 of Ivezić et al. (2008), which was calibrated using low metallicy globular clusters, and we applied to the 27 000 sources in our catalog with [Fe/H]< -0.5. Finally, 3D velocities in the galactic reference frame, V_R, V_ϕ, V_z, were derived by assuming $R_\odot$ = 8 kpc and the LSR velocity from Dehnen & Binney (1998).

3.1. Kinematic distribution

The velocity distribution, V_ϕ vs. V_R, of this kinematic sample is shown in Fig. 2 where the disk and halo populations are evident. In Table 1 we present the mean velocities and dispersions of stars with -0.7 <[Fe/H]< -0.5 and [Fe/H]< -1.8 which correspond to the metallicity ranges dominating in thick disk and halo stars, respectively. Although a more detailed analysis is mandatory, these results support (1) a mild prograde rotation, V_ϕ = 20-30 kms^{-1}, for the inner halo, and (2) a vertical rotation velocity gradient for the thick disk.

3.2. Searching for substructures

Motivated by results from high resolution CDM simulations and the previous analysis using the Beers et al. (2000) catalog of non-kinematically selected metal-poor stars (Re Fiorentin et al. 2005), we started using this sample to explore the stellar halo of the Milky Way and look for kinematic substructures. In order to identify moving groups, we derive integrals of motion in an axisymmetric

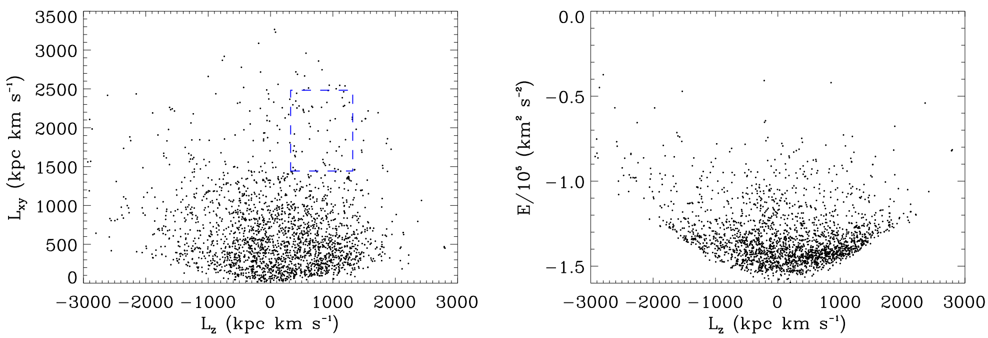

Fig. 3. Distribution of the selected halo stars with $D < 3$ kpc in the space of adiabatic invariants. The box highlights the location of the kinematic streams identified by Helmi et al. (1999).

potential, namely the energy, E, and the components of the angular momentum perpendicular L_{xy} and parallel L_z to the symmetry axis of the Galactic plane; moreover, the metallicity [Fe/H], is taken as an additional dimension in parameter space which is well suited to characterize their signatures.

Figure 3 shows the distribution of a subsample of halo stars ([Fe/H] < -1.8) within 3 kpc of the Sun in such space of adiabatic invariants, i.e. the components of the angular momentum perpendicular L_{xy} and parallel L_z to the symmetry axis of the Galactic plane, and energy. The box corresponds to the location of the kinematic stream identified by Helmi et al. (1999) and could indicate, among a wider sample, additional subdwarf members.

More than that, it appears clearly that the sample is not smoothly distributed over all the parameter space, but clustered. Preliminary results (Re Fiorentin et al. in preparation) confirm statistical evidence for discrete overdensities. By examination of their intrinsic properties, we suggest that they may be possible fossil signatures of past mergers or other accretion events.

Acknowledgements. The authours acknowledge the financial support of INAF through the PRIN 2007 grant n. CRA 1.06.10.04 "The local route to galaxy formation". Support through the Marie Curie Research Training Network ELSA (European Leadership in Space Astrometry) under contract MRTN-CT-2006-033481 to P.R.F. is also thankfully acknowledged.

References

Abazajian, K.N., Adelman-McCarthy, J.K., Agüeros, M.A., et al. 2009, ApJS, 182, 543
Andrei, A., Souchay, J., Zacharias, N., et al. 2009, A&A, in preparation
Beers, T.C., Chiba, M., Yoshii, Y., et al. 2000, AJ, 119, 2882
Dehnen, W., & Binney, J. 1998, MNRAS, 298, 387
Helmi, A., White, S.D.M., de Zeeuw, P.T., & Zhao, H.S. 1999, Nature, 402, 53
Ivezić, Ž., Sesar, B., Jurić, M., et al. 2008, ApJ, 684, 287
Lasker, B.M., Lattanzi, M.G., McLean, B.J., et al. 2008, AJ, 136, 735
Munn, J.A., Monet, D.G., Levine, S.E., et al. 2003, AJ, 127, 3034
Pier, J.R., Munn J.A., Hindsley, R.B, et al. 2003, AJ, 125, 1559
Re Fiorentin, P., Helmi, A., Lattanzi, M.G., & Spagna, A. 2005, A&A, 439, 551
Yanny, B., Rockosi, C., Newberg, H.J., et al. 2009, AJ, 137, 4377